JUSTC

Article

http://justc.ustc.edu.cn

Received: January 05, 2022; Accepted: March 19, 2022

Deployable boom for Mars Orbiter Magnetometer onboard Tianwen-1

Manming Chen[1,2], Zonghao Pan[1,2] ✉, Tielong Zhang[1,2,3] ✉, Xinjun Hao[1,2], Yiren Li[1,2], Kai Liu[1,2], Xin Li[1,2], Yuming Wang[1,2], Chenglong Shen[1,2], Hong Chen[4], Zhongwang Wang[4], and Xiu Qiang[5]

[1]*School of Earth and Space Sciences, University of Science and Technology of China, Hefei 230026, China;*
[2]*CAS Center for Excellence in Comparative Planetology, Hefei 230026, China;*
[3]*Space Research Institute, Austrian Academy of Sciences, Graz A-8042, Austria;*
[4]*Shanghai Institute of Aerospace System Engineering, Shanghai 201109, China;*
[5]*Shaanxi Applied Physics and Chemistry Research Institute, Xi'an 710061, China*

✉Correspondence: Zonghao Pan, E-mail: zhpan@ustc.edu.cn; Tielong Zhang, E-mail: tlzhang@ustc.edu.cn

Graphical abstract

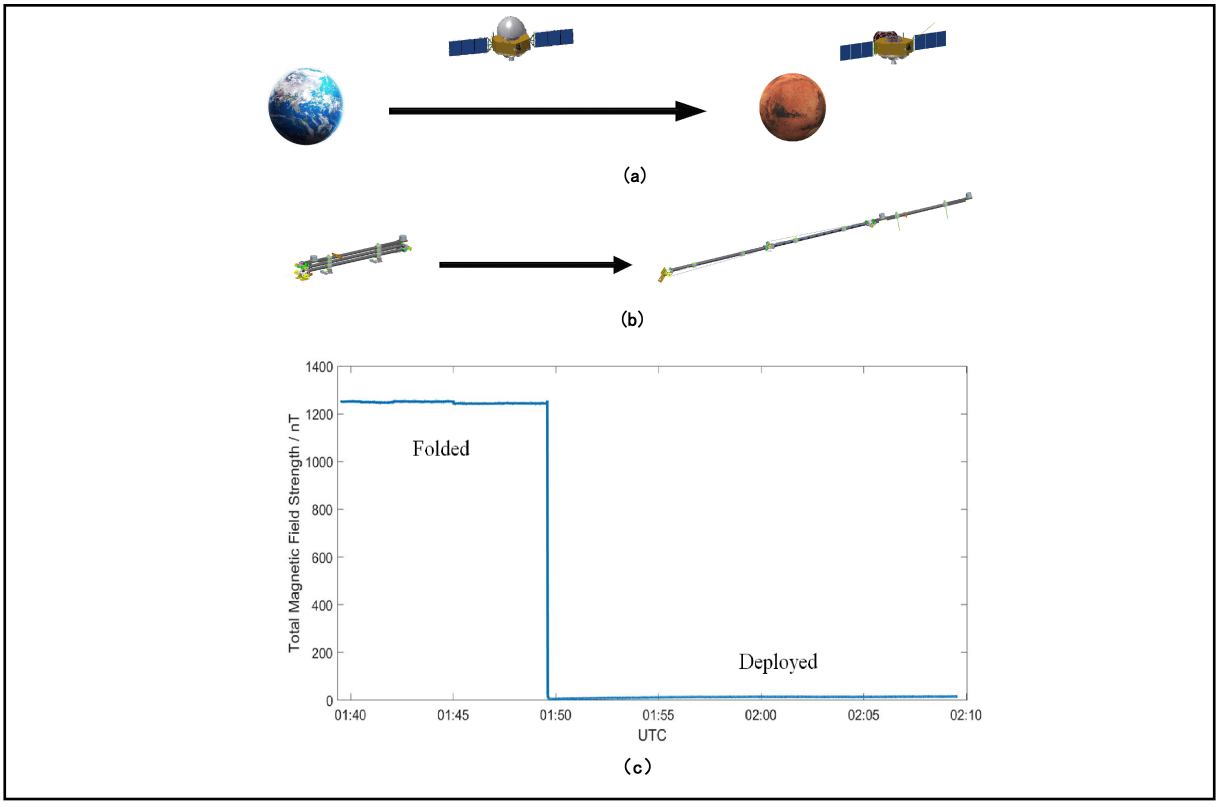

The deployable boom functioned normally and is consistent with the design expectations after long storage from Earth to Mars.

Public summary

■ The deployable boom is an essential component for China's first near-Mars space magnetic field exploration.

■ The deployable boom was folded and stowed for more than 300 days in space in cold environments before deployment.

■ The boom is accomplished with high reliability, short development and fabrication cycle under system constraints.

Citation: Chen M M, Pan Z H, Zhang T L, et al. Deployable boom for Mars Orbiter Magnetometer onboard Tianwen-1. *JUSTC*, **2022**, 52(5): 7. DOI: 10.52396/JUSTC-2022-0001

JUSTC

Article

http://justc.ustc.edu.cn

Received: January 05, 2022; Accepted: March 19, 2022

Deployable boom for Mars Orbiter Magnetometer onboard Tianwen-1

Manming Chen[1,2], Zonghao Pan[1,2] ✉, Tielong Zhang[1,2,3] ✉, Xinjun Hao[1,2], Yiren Li[1,2], Kai Liu[1,2], Xin Li[1,2], Yuming Wang[1,2], Chenglong Shen[1,2], Hong Chen[4], Zhongwang Wang[4], and Xiu Qiang[5]

[1]*School of Earth and Space Sciences, University of Science and Technology of China, Hefei 230026, China;*
[2]*CAS Center for Excellence in Comparative Planetology, Hefei 230026, China;*
[3]*Space Research Institute, Austrian Academy of Sciences, Graz A-8042, Austria;*
[4]*Shanghai Institute of Aerospace System Engineering, Shanghai 201109, China;*
[5]*Shaanxi Applied Physics and Chemistry Research Institute, Xi'an 710061, China*

✉Correspondence: Zonghao Pan, E-mail: zhpan@ustc.edu.cn; Tielong Zhang, E-mail: tlzhang@ustc.edu.cn

Cite This: *JUSTC*, **2022**, 52(5): 7 (7pp)

Read Online

Abstract: A more than 3 m-long deployable boom is an essential component of the Mars Orbiter Magnetometer (MOMAG) onboard the orbiter of Tianwen-1. The boom was developed to place fluxgate magnetometer (FGM) sensors away from the satellite to reduce the influence of the satellite magnetic field. It was designed as an articulated spring-driven deployable mechanism for single-shot deployment. Functionality, reliability and system constraints are fully considered in the boom design. Mechanical analyses and proof tests show that the boom has sufficient safety margin to withstand environmental conditions, even in the worst cases. After a long voyage from Earth to Mars, the boom was deployed successfully on May 25, 2021. A full deployment was performed in about 4.6 s, sending the two sensors to distances of 3.19 m and 2.29 m respectively, away from the orbiter. After deployment, the field from the orbiter decreased from 1250 nT to less than 6 nT at the sensor mounted at the tip of the boom. The MOMAG boom provides valuable engineering experience for the development of deployable structures stowed for long periods in cold temperatures in space missions.

Keywords: spacecraft boom; fluxgate magnetometers; Mars exploration; Tianwen-1

CLC number: V447 **Document code:** A

1 Introduction

China's first Mars exploration mission —Tianwen-1, was launched on July 23, 2020 in Wenchang, Hainan Province. The probe consists of an orbiter, a lander and a rover. After more than six-month journey, the probe was captured by Mars on February 10, 2021 and on May 15, 2021, the lander and rover successfully landed on Mars. Exploration of Mars is one of China's deep space exploration plans and will become a significant landmark project. It will advance our understanding of the origin, evolution and characteristics of the planet, and promote the development of space science and technology[1, 2].

The Mars Orbiter Magnetometer (MOMAG) is one of the seven scientific payloads onboard the Mars orbiter of Tianwen-1, and serves the mission of analyzing Martian ionosphere, plasma environment and atmospheric escape processes by measuring the ambient magnetic field in the near-Mars space[2–4]. It consists of two fluxgate magnetometer (FGM) sensors, an electronic box and a deployable boom. Unlike Earth, Mars has no global magnetic field[5, 6] and magnetic cleanliness programs on the orbiter are somewhat limited because of spacecraft operational considerations and other instrument needs. However, the influence of satellite magnetic fields can be weakened if the sensors are placed away from the spacecraft[7]. Deployable structures have been developed for various planetary magnetic-field investigation missions[8–11]. In this study, a deployable boom was developed to place the FGM sensors away from the orbiter. It is installed on the deck outside the orbiter, providing mechanical interfaces for FGM sensors and carrying cables from the sensors to the electronic box inside the orbiter. Fig. 1 shows the deployed state of the MOMAG boom on the orbiter.

An overview of the MOMAG boom is presented in this study. An analysis of the boom mission is described first. Then the boom design is described in detail, followed with the verification of proof and ground tests. In the end, the in-orbit operation shows that the boom functioned normally and is consistent with the design expectations.

2 Boom mission analysis

MOMAG will not start working until the boom deploys. The boom is folded in launch and transfer phase from Earth to Mars. After the target orbit is reached, the boom will not deploy until the lander successfully separates from the orbiter and lands on Mars. Fig. 2 illustrates the mission profile of MOMAG. A stowage of more than 300 days in a folded state in cold temperatures is a great challenge for the boom, requiring higher reliability, particularly in MOMAG mission where

DOI: 10.52396/JUSTC-2022-0001
JUSTC, **2022**, 52(5): 7

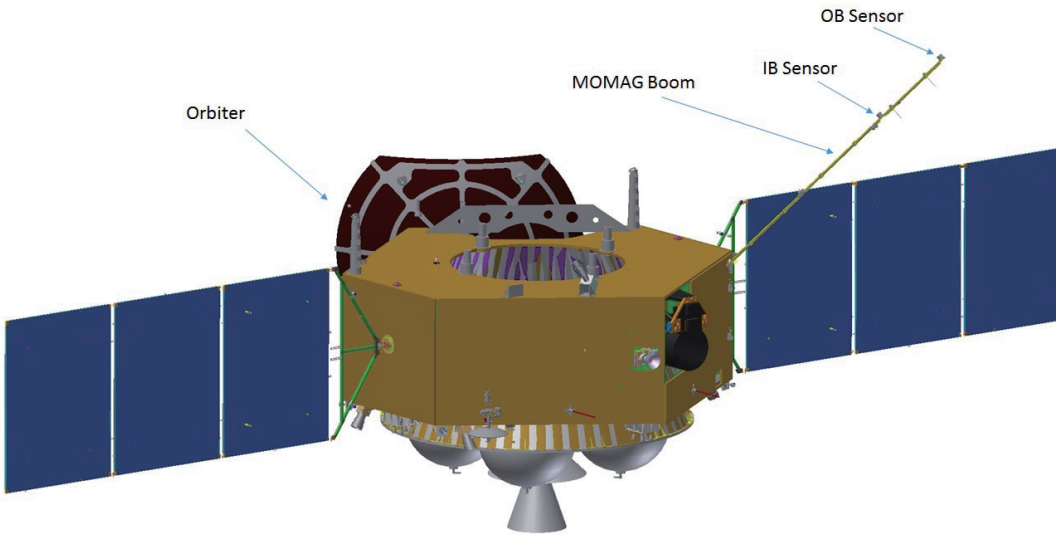

Fig. 1. A CAD model of deployed MOMAG boom on the Mars Orbiter of Tianwen-1.

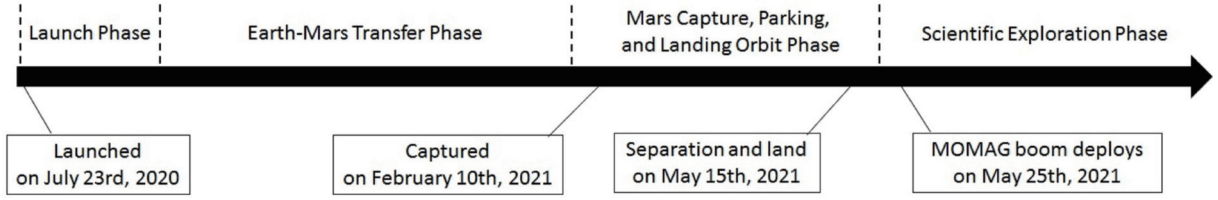

Fig. 2. Mission profile of MOMAG.

the successful boom deployment is a critical event.

A variety of mission requirements and system constraints were considered in the boom design. The mass of the boom has to be strictly no more than 4 kg and the boom size in folded state must be within 1.2 m long and 0.3 m high to avoid interference with the launch vehicle fairing and descent module in which the Mars rover and landing infrastructures are carried. Interference with other instruments on the same deck must also be avoided during deployment. Thus, the deployed boom length is constrained. In addition, because solar arrays are mounted on the nearby deck, the pointing of the boom must be designed to ensure that the FGM sensors could be placed as far away as possible to minimize the influence of satellite magnetic fields.

Additionally, the boom must survive the mechanical loads from launch, orbit transfer and satellite attitude control. Installed outside the orbiter, the boom must also survive thermal cycling between +80 ℃ and −180 ℃.

3 Boom design

The boom for MOMAG was developed as an articulated, spring-driven deployable mechanism for single-shot deployment. It consists of three boom limbs (inner, middle and outer limbs), three pairs of hinges (two pairs of elbow hinges and a pair of root hinges), a base assembly and two sets of hold-down and release systems. As illustrated in Fig. 3, the outer limb is attached to the middle limb by a pair of elbow hinges, and an identical attachment lies between the middle and inner limbs. The inner limb is hinged to the base assembly via a pair of root hinges. In the folded configuration, the boom is

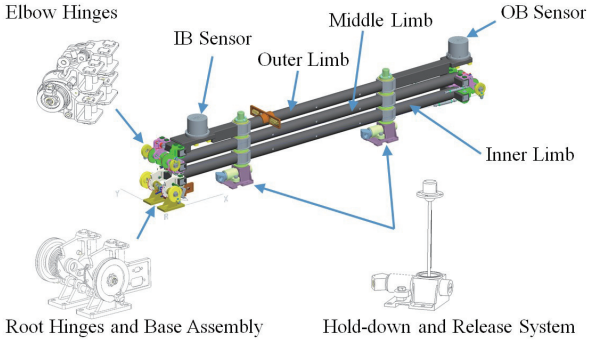

Fig. 3. CAD model of MOMAG boom in folded configuration.

1.11 m long. Once deployed, the total length of the boom is as long as 3.19 m from the tip to the base assembly, and the angle between the boom and the deck is 135° with an error within ±1° to ensure that the FGM sensors are placed farthest away from the solar array and the orbiter. The outboard FGM sensor (OB Sensor) lies at the tip of the deployed boom and the inboard FGM sensor (IB Sensor) is positioned 0.9 m along the boom away from the OB Sensor. The outputs of the two sensors function as a gradiometric method to subtract unwanted magnetic disturbances from the ambient field[12–14]. A summary of MOMAG boom specification is presented in Table 1.

3.1 Boom configuration

3.1.1 Boom limbs

The boom limbs are fabricated via moulding, filament winding and tube rolling processes with carbon fiber reinforced

DOI: 10.52396/JUSTC-2022-0001
JUSTC, **2022**, 52(5): 7

Table 1. Summary of MOMAG boom specification.

Property	Requirement	Performance	Note
Mass	⩽4 kg	3.945 kg	
Stowed length	⩽1.2 m	1.11 m	
Deployed length	⩾3 m	3.19 m	
Deployment time	⩽8 s	4.3 s	Mean value of ground measurements
Deployment angle	135°±1°	134.96°	Mean value of ground measurements
Temperature range	−180 ℃ to +80 ℃	−195 ℃ to +95 ℃	Temperature of thermal cycling test

plastics (CFRP) MJ55 and T700S owing to their high stiffness and strength-to-weight ratio. The high stiffness of CFRP easily satisfies the mechanical requirements, and its low density minimizes the mass budget of the boom. Each limb could reach as long as 1.01 m long with an outer diameter of 30 mm. Owing to weight concern, the inner diameters of boom limbs are designed with respect to the stiffness and frequency requirements. The inner and middle limbs provide interfaces for hinges at both ends while the outer limb provides interfaces for both FGM sensors and hinges, as presented in Fig. 4. In addition, a connector bracket made of aluminum alloy is also fixed on the outer limb, so that the FGM sensors could be easily removed for testing. Two bushings made of reinforced aluminum matrix composites are distributed along each limb to provide access for hold-down titanium rods.

3.1.2 Hinges

The hinges are spring-driven with a latch mechanism for single-shot deployment, which are mainly made of aluminum and titanium alloys. In the folded configuration, the energy from the shape change of the volute spiral spring is stowed and a torque of 0.7 N·m is delivered by a single hinge. When fully deployed, the hinges are latched against an end stop, providing sufficient stiffness and preventing back-driving. The root hinges are integrated into the base assembly which provides interfaces for installation on the deck.

In addition, two sets of closed cable loops (CCLs), which are derived from the solar arrays' synchronization system, are used to avoid uncontrolled release of spring energy into the system during deployment. Thus, the three pairs of hinges are opened in a synchronized manner until the end stops are reached and the hinges are latched. Therefore, there will be no variation in the deployment trajectory. A typical deployment process is illustrated in Fig. 5.

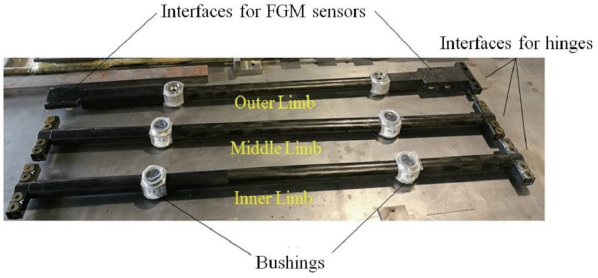

Fig. 4. Picture of boom limbs for flight model.

3.1.3 Hold-down and release system

The hold-down and release system consists of a holding bracket, a hold-down titanium rod, an initiating explosive device (IED) and a shock absorber cap (SAC). Fig. 6 is the CAD model of a set of hold-down and release system. Two sets are required for the deployment of the boom.

The holding brackets are made of magnesium alloy type ZK61M because of weight concern and mounted on the deck of the spacecraft. First, each IED is mounted on a holding bracket. Then a hold-down titanium rod with a diameter of 3.5 mm is passed through the bushings and IED. Finally, the titanium rod is screwed to the bottom of the holding bracket. Thus, the boom is held down in folded configuration, as shown in Fig. 3. IED is a release mechanism based on the principle that a cutting knife is pushed out by the explosion inside the shell to cut the titanium rod. The cutting is

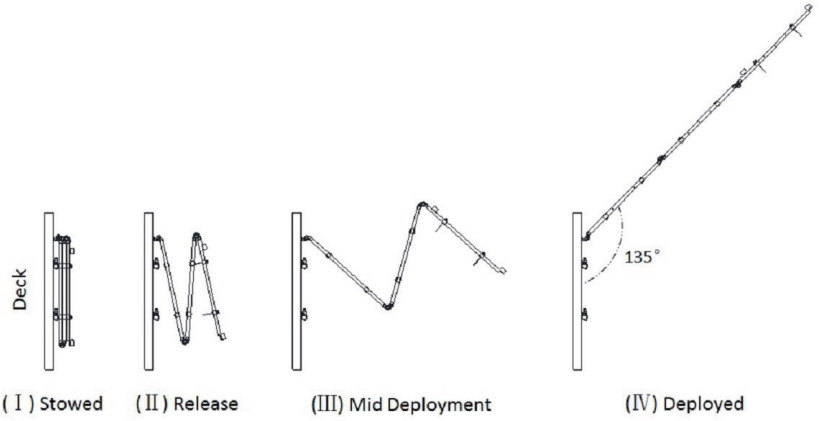

Fig. 5. MOMAG boom deployment process.

DOI: 10.52396/JUSTC-2022-0001
JUSTC, **2022**, 52(5): 7

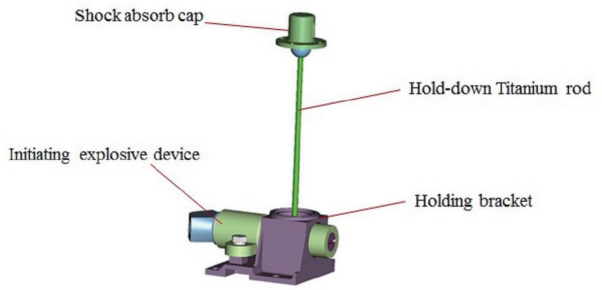

Fig. 6. CAD model of a set of hold-down and release system.

executed within 40 ms and SAC is used to release the shock caused by the cutting. The boom will be deployed as soon as the cutting is done.

3.1.4 Mechanical analysis

Regarding weight concern and high reliability, CFRP, aluminum, titanium and magnesium alloys are the main materials chosen for the boom and its structure design should ensure that the boom is robust enough to withstand mechanical loads in harsh conditions. The finite element method is applied in the boom mechanical analysis. Fig. 7 presents the finite element models (FEM) of the MOMAG boom and hinges in deployed state. The analytical results listed in Table 2 show that both the boom limbs and hinges (elbow and root hinges) have sufficient safety margins of strength to provide high reliability for the boom even in the worst mechanical environments after deployment.

The MOMAG goes through several phases during flight. Among them, the greatest mechanical load could reach no more than 2.5 m/s^2 caused by a propulsion force of 3000 N

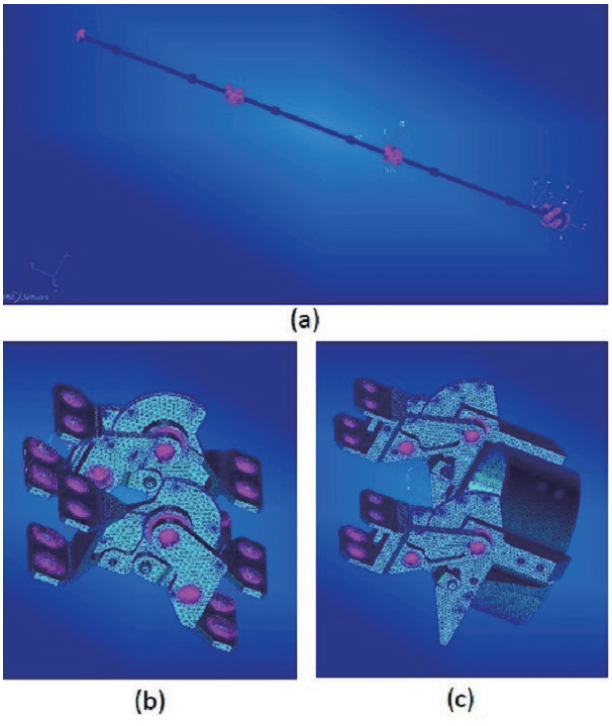

Fig. 7. Finite element models (FEM) of deployed boom for mechanical analysis. (a) FEM of deployed boom; (b) FEM of elbow hinges; (c) FEM of root hinges.

Table 2. Results of boom strength analysis.

Component	Stress tensor (maximum)	Safety margin	
		Requirement	Analytical result
Root hinges	132 MPa	>0	2.17
Elbow hinges	42.7 MPa	>0	8.80
Boom limbs	70.1 MPa	>0.25	11.07

during the Earth-Mars orbit transfer. However, the boom won't deploy until the spacecraft reaches the scientific exploration orbits around the Mars, in which case the propulsion force could be just about one or several hundred newtons. A ground-verification experiment is conducted to test the pointing stability of the boom. The test scheme is illustrated in Fig. 8. After the deployment of the boom, a mechanical load is applied along the X or Z direction with an acceleration of 2.5 m/s^2, simulating the greatest mechanical load in orbit. Position 0 represents the designed pointing position of the boom, whereas position 1 and 2 represent the oscillation of boom caused by the mechanical load. The results show that the boom could stop at position 0 within 10 s, and the oscillation amplitude is less than 10 cm.

3.2 Thermal and cable design

The boom limbs, holding brackets and IEDs are all protected with multilayer insulation (MLI) blankets to reduce thermal gradients. A small, 2-watt heater is situated on each holding bracket to improve the thermal stability of the IEDs. And a thermistor is also attached in the vicinity of each IED to monitor its temperature. To reduce the thermal conduction between the boom and FGM sensors, a 5 mm-thick heat-insulated pad is placed between each sensor and the boom. MLI blankets are also used to cover the sensors and cables for thermal protection.

The FGM sensors and electronic box are connected by two long cables which are protected by a woven sleeve and braid shield for electromagnetic interference and durability. Each cable is more than 4 m long and routed along the boom as shown in Fig. 9. For the benefit of test and operation, each

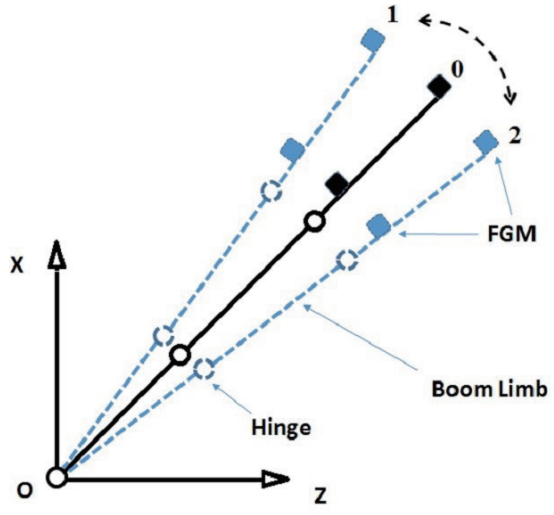

Fig. 8. Scheme of boom pointing stability test.

DOI: 10.52396/JUSTC-2022-0001
JUSTC, **2022**, 52(5): 7

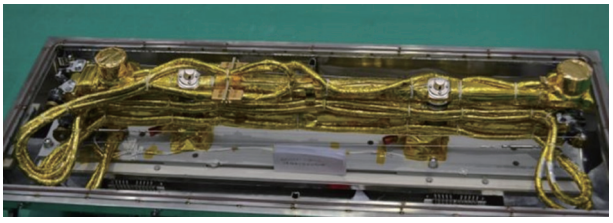

Fig. 9. Flight model of MOMAG boom with FGM sensors and cables.

cable is divided into 2 parts: A pig tail fixed into the sensor and a connecting cable as long as 3.5 m with connectors at both ends. Cable supports are used at both the elbow and root hinges to allow free hinge rotations and to avoid unexpected interference with other parts of the boom during deployment.

4 Proof tests

As the hinges and IEDs play a key role in the boom deployment, proof tests are necessary to provide adequate reliability for boom deployment after long-term storage in cold environments. Stowed hinges were soaked in liquid nitrogen (LN) for one year and function test was conducted afterward. The test showed that the hinges could deploy and be locked normally after one year of storage in LN, as shown in Fig. 10. And a long-term storage test was also conducted for the hold-down and release system. Two sets of hold-down and release systems were stored in vacuum state at certain temperatures to simulate the environment in orbit for more than 10 months. The hold-down and release systems functioned normally: both IEDs cut titanium rods within 40 ms, as shown in Fig. 11. Further function test for IED was also conducted by keeping

Fig. 10. Picture of function test for hinges after storage in LN for one year.

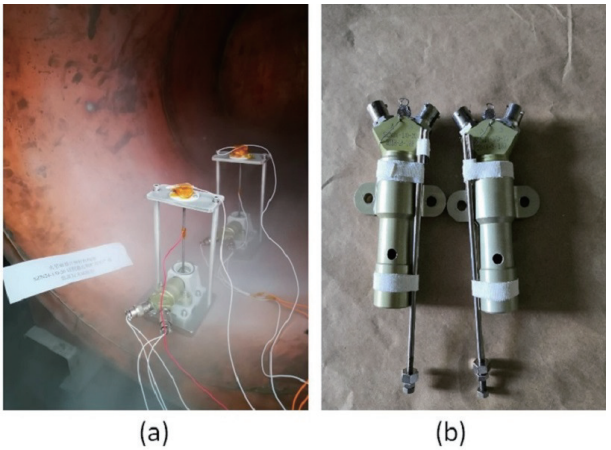

Fig. 11. Function test for hold-down and release systems after long-term storage. (a) Picture of hold-down and release systems ready for function test in the simulated environment; (b) Picture of IEDs and titanium rods after function test.

five IEDs stored at a temperature lower than −180 ℃ for about one year. All the IEDs worked normally, cutting the titanium rods within 40 ms. A picture of IED transections is presented in Fig. 12.

Because the FGM sensor cable was protected with a woven sleeve, braid shield and MLI blanket, each cable could reach 17.5 mm in diameter. The rigidity of cables, especially in cold environment, and its influence on the boom deployment are critical issues because the successful deployment is a vital mission event in our case. A verification test of sufficient torque margin for the hinges was conducted by deploying a pair of elbow hinges with cables of three times by soaking the whole apparatus in LN (−196 ℃), as presented in Fig. 13. The hinges deployed and locked normally within 1 s, thereby verifying the torque margin of the hinges.

5 Ground tests

After assembly of the boom, FGM sensors and cables, ground tests must be performed. When testing a deployable boom, the most critical issue is to prove that the boom will deploy successfully. However, it is not easy to test large deployable booms in a simulated space environment on the ground. The deployment test must verify the functionality of the boom, while wear and degradation brought up by the test should also be concerned. A horizontal deployment test scheme was developed, reviewed and implemented for our boom, as presented in Fig. 14.

The test was conducted in room ambient conditions. The boom was installed on a breadboard fixed on a truss. Floata-

Fig. 12. Picture of IED transections after function test.

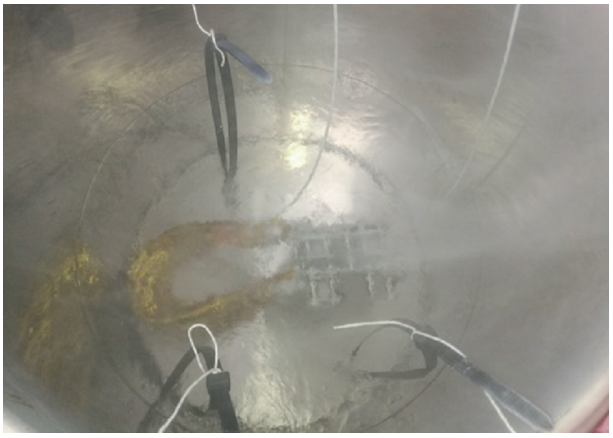

Fig. 13. Margin verification test of hinges with cables of three times.

DOI: 10.52396/JUSTC-2022-0001
JUSTC, **2022**, 52(5): 7

tion components were attached to boom limbs. Pressurized air through the floatation components creates a uniform air gap between the components and marble platform, offsetting the weight of the boom, sensors and cables. The air gap allows the floatation components to travel with little friction on the marble platform, and a constant, stable force is maintained for continuous weight offset during deployment. The repeatability of pre-launch deployment tests shows that the angle between the boom and deck lies within 135°±0.1°, and the deployment time is 4.3 s in average.

After the deployment test, the boom was folded and mounted on a vibration table and all three major directions were tested under sinusoidal and random vibrations. Following this, a thermal cycle test between −195 ℃ and +95 ℃ and a thermal vacuum test were performed. Then a post-test deployment was performed to verify the functionality of the boom. Fig. 15 shows the boom during environmental tests.

6 In-orbit operation

The boom was stowed at low temperature for more than 300 days since its launch. After separation of the orbiter and lander, the boom was deployed successfully on May 25, 2021. The boom deployed the full 3.19 m in approximately 4.6 s as predicted and tested. High-resolution time (32 Hz) data were recorded by both IB and OB sensors throughout the deployment. Fig. 16 shows the total magnetic field data output of each sensor throughout the deployment. In the folded configuration, the field is dominated by the spacecraft field. As the boom deploys and places the sensors away from the spacecraft, the magnetic field at the sensors decreases as expected. The measured field strength in the IB sensor decreased from 1360 nT to less than 163 nT, and the field strength in the OB sensor decreased from 1250 nT to less than 6 nT. The field magnitude is consistent with expectations for the near-Mars space. Field data observed later showed that the boom properties were consistent with the mechanical design expectations.

7 Conclusions

The MOMAG boom was developed to place the FGM sensors away from the Mars orbiter to minimize the influence of the satellite magnetic fields. It was designed, fabricated and

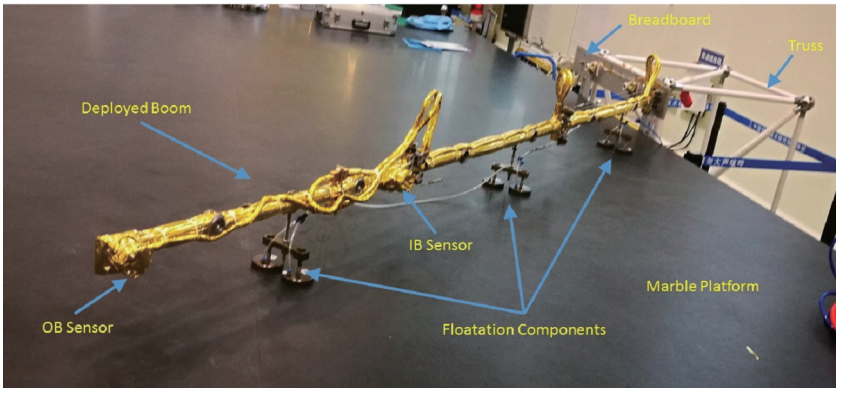

Fig. 14. Boom deployment test for flight model.

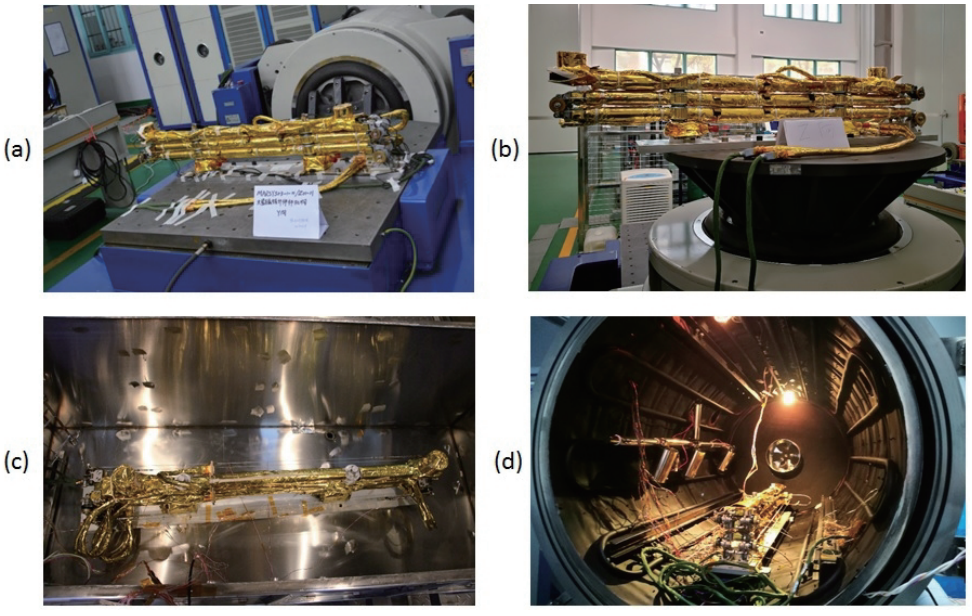

Fig. 15. Environmental tests for the boom. (a) and (b) are pictures of boom taken during vibration test in horizontal and vertical directions respectively. (c) and (d) are pictures taken during thermal cycle test and thermal vacuum test respectively.

DOI: 10.52396/JUSTC-2022-0001
JUSTC, **2022**, 52(5): 7

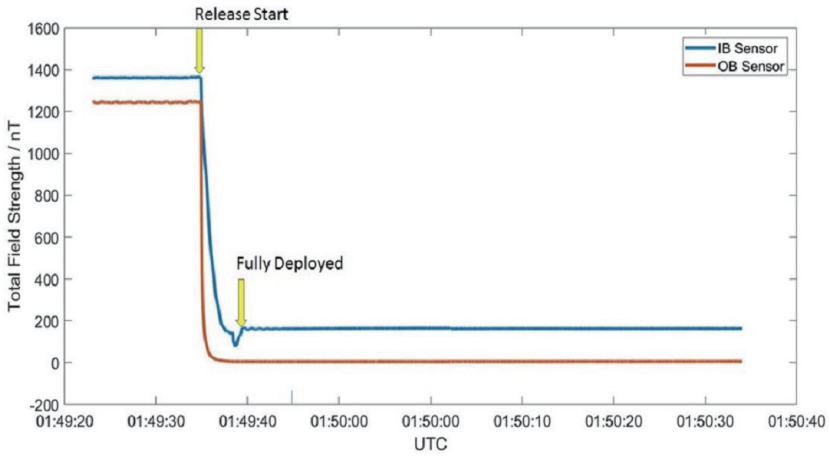

Fig. 16. Total magnetic field observed by both FGM sensors during boom deployment. Time is UTC.

tested under the requirements of functionality, reliability and system constraints. The boom was controlled within 4 kg and reaches 3.19 m once deployed. Proof and ground tests showed that the boom could function normally after long-term storage in a cold environment. It completed acceptance verification for use in flight in 2019 and deployed successfully on May 25, 2021. The field at both FGM sensors decreased as expected, and the boom appeared to be in good accord with the design expectation. It was predicated as a high-risk task with a short development and fabrication cycle. The MOMAG mission offers a unique opportunity to advance the functionality and reliability of deployable booms stowed for long periods in cold environments, providing reliable engineering technology of deployable booms for China's future space missions.

Acknowledgements

This work was financially supported by the Chinese National Space Administration (CNSA), the Strategic Priority Program (XDB41000000), the Key Research Program of Frontier Sciences (QYZDB-SSW-DQC015) and the Strategic Priority Program (XDB41030100) of the Chinese Academy of Sciences.

Thanks go to the entire MOAMG boom team at the University of Science and Technology of China and the Shanghai Institute of Aerospace System Engineering. Thanks also go to all the fraternities and experts whose advices and criticism helped make the boom robust enough to survive qualifications with high reliability.

Conflict of interest

The authors declare that they have no conflict of interest.

Biographies

Manming Chen is currently a doctoral candidate at the University of Science and Technology of China. His research interests focus on the development of magnetometers and magnetic shielding facilities.

Zonghao Pan is currently an engineer at the School of Earth and Space Sciences, University of Science and Technology of China (USTC). He received his Ph.D. degree in Space Physics from USTC. His research interests mainly focus on the space magnetic field investigation.

Tielong Zhang is Academician of International Academy of Astronautics, and is an expert in space science and planetary physics. He is also the chief designer of MOMAG mission. His research interests include planetary physics, exploration of deep space and development of space-based magnetometers.

References

[1] Ouyang Z Y, Xiao F G. Major scientific issues involved in Mars exploration. *Spacecraft Environment Engineering,* **2011**, *28* (3): 205–217.

[2] Li C L, Zhang R Q, Yu D Y, et al. China's Mars exploration mission and science investigation. *Space Science Reviews,* **2021**, *217*: 57.

[3] Li C L, Liu J J, Geng Y, et al. Scientific objectives and payload configuration of China's first mars exploration mission. *Journal of Deep Space Exploration,* **2018**, *5* (5): 406–413.

[4] Liu K, Hao X J, Li Y R, et al. Mars Orbiter Magnetometer of China's first mars mission Tianwen-1. *Earth Planet Physics,* **2020**, *4* (4): 384–389.

[5] Michaelis H, Motschmann U, Roatsch T, et al. Magnetic fields near Mars: First results. *Nature,* **1989**, *341*: 604–607.

[6] Acuna M H, Connerney J E P, Wasilewski P, et al. Magnetic field and plasma observations at Mars: Initial results of the Mars Global Surveyor Mission. *Science,* **1998**, *279* (5357): 1676–1680.

[7] Acuna M H. Space-based magnetometers. *Review of Scientific Instruments,* **2002**, *73* (11): 3717–3736.

[8] Zhang T L, Baumjohann W, Delva M, et al. Magnetic field investigation of the Venus plasma environment: Expected new results from Venus Express. *Planetary and Space Science,* **2006**, *54* (13-14): 1336–1343.

[9] Anderson B J, Acuna M H, Lohr D A, et al. The Magnetometer instrument on MESSENGER. *Space Science Reviews,* **2007**, *131*: 417–450.

[10] Connerney J E P, Espley J, Lawton P, et al. The MAVEN magnetic field investigation. *Space Science Reviews,* **2015**, *195*: 257–291.

[11] Connerney J E P, Benn M, Bjarno J B, et al. The Juno Magnetic Field investigation. *Space Science Reviews,* **2017**, *213*: 39–138.

[12] Ness N F, Behannon K W, Lepping R P, et al. Use of two magnetometers for magnetic field measurements on a spacecraft. *Journal of Geophysical Research,* **1971**, *76* (16): 3564–3573.

[13] Neubauer F M. Optimization of multimagnetometer systems on a spacecraft. *Journal of Geophysical Research,* **1975**, *80* (22): 3235–3240.

[14] Georgescu E, Auster H U, Takada T, et al. Modified gradiometer technique applied to Double Star (TC-1). *Advances in Space Research,* **2008**, *41* (10): 1579–1584.

DOI: 10.52396/JUSTC-2022-0001
JUSTC, **2022**, 52(5): 7